Supporting Information

Engineering of Heterojunction-Mediated Biointerface for Photoelectrochemical Aptasensing: Case of Direct Z-Scheme CdTe-Bi_2S_3 Heterojunction with Improved Visible-Light-Driven Photo-electrical Conversion Efficiency

Qian Liu[a], Juan Huan[b], Nan Hao[b], Jing Qian[b], Hanping Mao[*a] and Kun Wang[*b]

[a]*Key Laboratory of Modern Agriculture Equipment and Technology, School of Agricultural Equipment Engineering, Jiangsu University, Zhenjiang 212013, P.R. China*

[b]*School of Chemistry and Chemical Engineering, Jiangsu University, Zhenjiang 212013, P.R. China*

∗Corresponding author. Tel.: +86 511 88791800; fax: +86 511 88791708.

E-mail address: wangkun@ujs.edu.cn; maohp@ujs.edu.cn

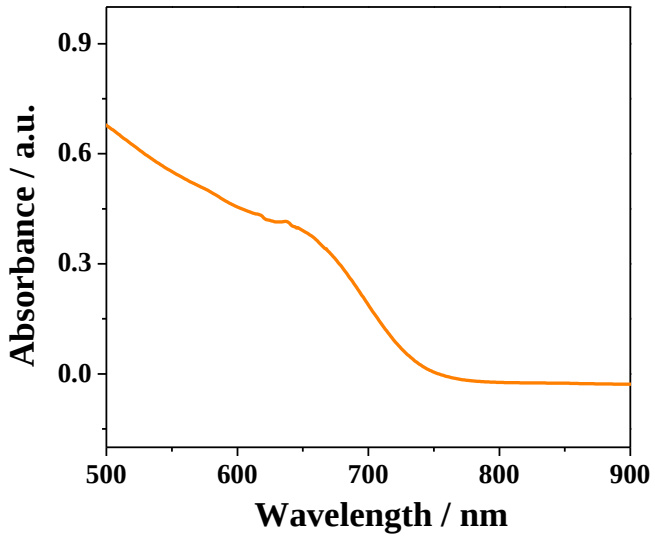

Figure S1 UV-vis spectrum of CdTe QDs solution.

Figure S1 showed the UV-Vis absorption spectrum of CdTe QDs. It is obvious that a wide absorption band around 660 nm was observed. According to the empirical equations as follows:[23]

$$D = (9.8127 \times 10^{-7})\lambda^3 - (1.7147 \times 10^{-3})\lambda^2 + (1.0064)\lambda - 194.84$$

$$C = \frac{A}{10043(D)^{2.12}L}$$

where D (nm) and C (M) are the size and concentration of CdTe QDs, respectively. λ (nm) is the wavelength of the first excitonic absorption peak, A is the absorbance at the peak position of the first exciton absorption peak for CdTe QDs, and L (cm) is the path length of the radiation beam. The size and the concentration of the CdTe QDs solution were estimated to be 4.6 nm and 1.5 μM by the empirical equations above.

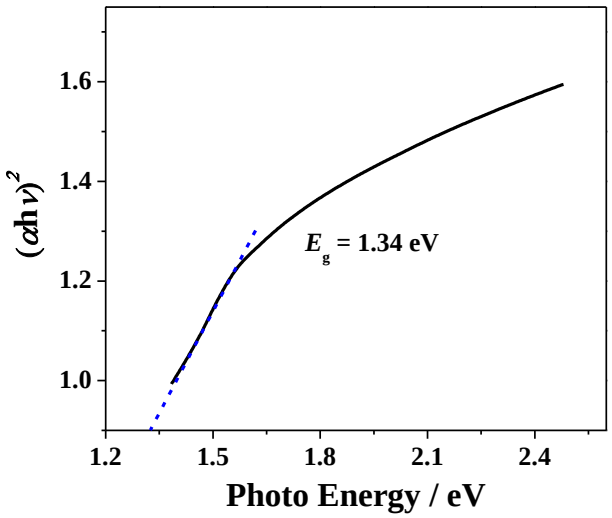

Figure S2 Tauc's plots to determine the band gap for Bi_2S_3 NRs.

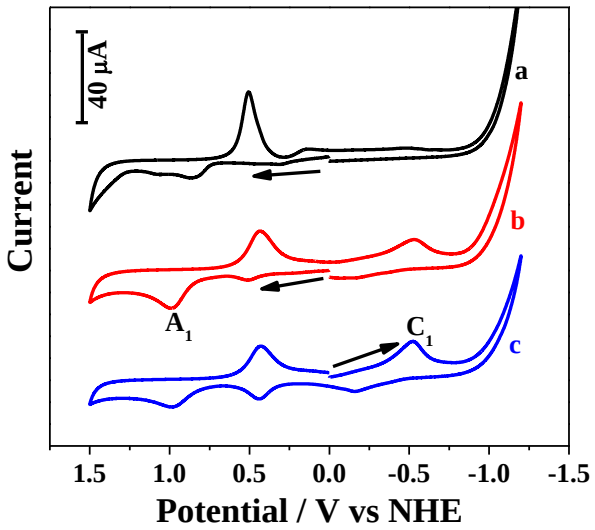

Figure S3 Cyclic voltammograms of gold disc electrode recorded in borate buffer solution in the absence (a) and presence of CdTe QDs (b, c); (b) First sweep toward a direction of positive potential (0→+1.5 V), (c) First sweep toward a direction of negative potential (0→−1.2 V).

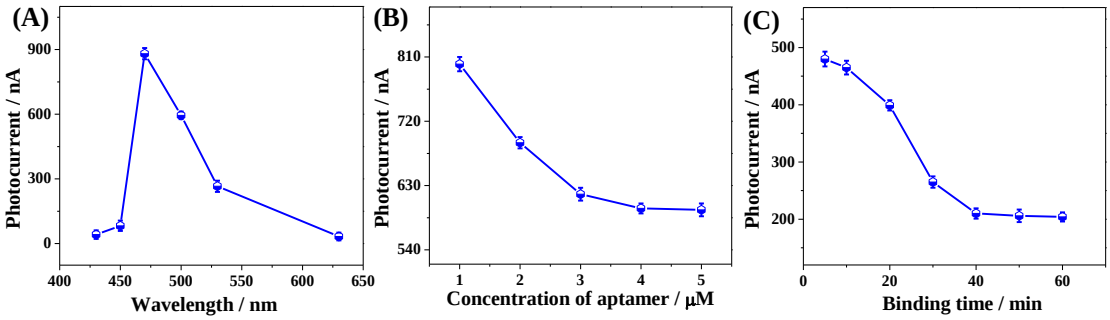

Figure S4 Effects of (A) accessory light source with different wavelength (B) the aptamer concentration and (C) binding time of MC-LR with the aptamer on the photocurrent response of the aptasensor.

Table S1 Zeta potential results of CdTe QDs, Bi_2S_3 NRs and CdTe-Bi_2S_3 heterojunction.

Material	CdTe QDs	Bi_2S_3 NRs	CdTe-Bi_2S_3
Zeta potential (mV)	–39.7	+19.9	–35.5

Table S2 Analytical performance of different sensing methods for MC-LR.

Methods	**Linear Range**	**Detection limit**	**References**
PEC aptasensor	0.1~1000 pM	0.03 pM	36
Electrochemical aptasensor	0.1~1000 pM	1.9 pM	38
Colorimetric aptasensor	0.1~250 nM	0.05 nM	39
Fluorescence aptasensor	0.01~50 nM	0.002 nM	40
Impedimetric immunosensor	0.01~100 nM	0.04 nM	41
PEC aptasensor	0.01-100 pM	0.005 pM	This work

Table S3 Analysis of real water samples with different concentrations of MC-LR (n = 3).

	Tap Water			**River water**		
Added/pM	Found/pM	Recovery/%	RSD/%	Found/pM	Recovery/%	RSD/%
0.2	0.19±0.02	95.0	5.7	0.22±0.02	110	5.3
2	1.93±0.17	96.5	5.4	2.13±0.11	106.5	6.8
20	19.1±1.24	95.5	6.1	21.6±1.02	108	6.5

References

(23) Wang, W. J.; Hao, Q.; Wang, W.; Bao, L.; Lei, J. P.; Wang, Q. B.; Ju, H. X. Quantum Dot-functionalized Porous ZnO Nanosheets as a Visible Light Induced Photoelectrochemical Platform for DNA Detection. *Nanoscale* **2014**, *6*, 2710–2717.